Structural Evolution of Cr(III) Polymeric Species at the γ-Al2O3/Water Interface

ARTICLE *in* ENVIRONMENTAL SCIENCE AND TECHNOLOGY · NOVEMBER 2000

Impact Factor: 5.33 · DOI: 10.1021/es9914285

3 AUTHORS, INCLUDING:

Jeffrey P Fitts
Princeton University
76 PUBLICATIONS **893** CITATIONS

SEE PROFILE

Environ. Sci. Technol. **2000**, *34,* 5122−5128

Structural Evolution of Cr(III) Polymeric Species at the γ-Al_2O_3/Water Interface

JEFFREY P. FITTS,[†] GORDON E. BROWN, JR.,*[,†,‡] AND GEORGE A. PARKS[†]

Surface and Aqueous Geochemistry Group, Department of Geological and Environmental Sciences, Stanford University, Stanford, California 94305-2115, and Stanford Synchrotron Radiation Laboratory, P.O. Box 4349, Stanford, California 94309

We have characterized the structure of the predominant Cr(III) species present at the γ-Al_2O_3/water interface as a function of equilibration time and Cr(III) surface loading using X-ray absorption fine structure (XAFS) spectroscopy. The spectroscopic measurements span two distinct time periods of Cr(III) uptake. During the initial period (<2 h), which is characterized by rapid uptake, Cr(III) monomers form inner-sphere complexes on the γ-Al_2O_3 surface by bonding to at least two surface functional groups. During the second period (ranging from 2 h to 1 week), significant quantities of Cr(III) continue to be removed from solution, but sorption proceeds at a greatly reduced rate. The XAFS spectra collected during the period of slow uptake show an increase in scattering contributions from neighboring Cr(III) atoms with increasing equilibration time. The inferred structural changes are consistent with a progression from hydroxo-bridged Cr(III) dimers to higher-order polymers. In combination with spectroscopic evidence, which shows that monomeric Cr(III) species are the only significant reactants in solution, the observed evolution of Cr(III) surface species suggests that chemical bonding between adsorbed Cr(III) ions and γ-Al_2O_3 surface functional groups enhances Cr(III) polymerization. The proposed reaction sequence has important implications for surface complexation modeling used to predict Cr(III) partitioning by hydroxide sorbents in wastewater treatment and contaminant migration scenarios.

Introduction

Cr-containing waters released as a result of historic and current mining and industrial practices threaten a variety of aquatic ecosystems (*1*, *2*). The aqueous concentration of Cr(III) in these ecosystems is typically controlled by sorption processes occurring on aluminosilicate clay minerals and manganese, iron, and aluminum (hydr)oxides (*2*, *3*). These sorption processes include adsorption/desorption, diffusion, polymerization, and precipitation/dissolution. How these processes affect the aqueous concentration of Cr(III) is of great concern because relative to sorbed Cr(III), dissolved Cr(III) is more bioavailable and susceptible to oxidatitive transformation than the more toxic and more mobile Cr(VI) species (*2*, *3*). The surface complexation and reactive transport models used to predict Cr(III) concentrations in contaminated aquifers and wastewaters require greatly simplified representations of Cr(III) sorption phenomena. However, simplifications that fail to incorporate important sorption phenomena can lead to grossly inaccurate predictions. Therefore, a fundamental understanding of the mechanisms governing Cr(III) sorption onto metal (hydr)oxides is important for assessing both the potential hazard Cr contamination presents to an aquatic ecosystem and the removal efficiency of a wastewater treatment method.

Macroscopic uptake studies have demonstrated that Cr(III) sorbs strongly to most metal (hydr)oxide phases above pH 4. However, Cr(III) uptake is dynamic, attaining a quasi-equilibrium state at metal (hydr)oxide/water interfaces only after long equilibration times. Kinetic investigations have established that Cr(III) uptake proceeds in two distinct stages (*4*, *5*). An initial period of rapid uptake (typically less than 2 h) is followed by a period of slow uptake (days to weeks). In addition, the rates of Cr(III) uptake during both periods increase with the hydroxide ion concentration. Microscopic and spectroscopic investigations of Cr(III) sorption on silica (*6*, *7*), iron (hydr)oxides (*6*, *8*), and hematite (*9*) have focused on the sorption products formed from solutions near saturation with respect to chromium hydroxide and/or after long equilibration times (greater than 5 days). The general conclusion from these studies is that the composition and structure of the surface determines the morphology and structure of the sorption product. Specifically, Cr(III) forms discrete chromium(III) hydroxide clusters on silica and chromium(III) hydroxide precipitates that mimic the underlying surface structure on iron (hydr)oxides and magnetite (*10*). As a result of these spectroscopic findings, recent efforts to model Cr(III) uptake have considered surface precipitation (*11*). However, to derive kinetic and thermodynamic constants that are applicable over a wide range of solution conditions, chemical reactions must be proposed that accurately reflect the mechanisms responsible for Cr(III) uptake (*12*, *13*). Spectroscopic information about the intermediate sorption products formed prior to surface precipitation is needed to derive accurate descriptions of these chemical reactions.

The relatively slow kinetics of Cr(III) uptake presents a unique opportunity to study the evolution of sorption products with conventional spectroscopic methods. Karthein et al. (*14*) studied Cr(III) sorption on γ-Al_2O_3 as a function of equilibration time with electron paramagnetic resonance (EPR) spectroscopy. The EPR spectra indicate a gradual change in the local coordination environment of adsorbed Cr(III) with increasing equilibration time. However, the authors were unable to assign definitively the observed trend to either hydrolysis of adsorbed Cr(III) or polynuclear complex formation. As a molecular-scale probe of local coordination environments of metal ions (within a 5-Å radius), X-ray absorption fine structure (XAFS) spectroscopy is well suited for detecting the onset of Cr(III) polymerization, assuming that metal ions in the sorbent are sufficiently different from Cr in their electron backscattering amplitude and phase shift, which is clearly the case for Al in γ-Al_2O_3. In addition, the bonding environment of Cr(III) ions located at the metal (hydr)oxide/water interface can be inferred from the fit parameters (coordination number, distance to neighboring atomic shells, disorder parameter) of the extended XAFS (EXAFS) spectra.

The present XAFS investigation examines the predominant Cr(III) species formed at the γ-Al_2O_3/water interface during the fast and slow periods of uptake from a chromium(III) nitrate solution. On the basis of the local structure of the

* To whom correspondence should be addressed to at Stanford University, Bldg. 320, Rm. 118. Phone: (650)723-9168; fax: (650)-725-2199; e-mail: gordon@pangea.stanford.edu.

[†] Stanford University.

[‡] Stanford Synchrotron Radiation Laboratory.

10.1021/es9914285 CCC: $19.00
Published on Web 11/10/2000

predominant Cr(III) surface species, chemical reactions are proposed and potential sorption mechanisms are discussed. We find that monomeric Cr(III) species form inner-sphere complexes during the period of fast uptake and that hydroxo-bridged Cr(III) dimers and higher-order oligomers form at longer equilibration times. Finally, we discuss the implications of these findings for models used to predict the sorption capacity of metal (hydr)oxides and the stability of surface-bound Cr(III) against remobilization and potential oxidation to Cr(VI).

Experimental Section

Materials. The γ-Al_2O_3 powder used in this study was purchased from Degussa under the brand name Aluminum Oxide C. The manufacturer reported the purity (99.6%) and surface area (N_2 BET 100 $\pm$ 15 m^2/g). The γ-Al_2O_3 was preequilibrated with a 0.1 M $NaNO_3$ solution for 24 h prior to reaction with a metal-bearing solution in order to swamp the surface with the chosen electrolyte and hydrolyze surface functional groups. A recent diffuse reflectance FTIR study demonstrated that γ-Al_2O_3 is not stable in aqueous suspensions and that the surface transforms to a bayerite-like phase (β-$Al(OH)_3$) (*15*). Although this transformation has been shown to continue for up to 1 month (*16*, *17*), results from a recent study (*18*) suggest that ligand exchange rates at the most reactive hydroxyl groups (terminal and bridging) of octahedral Al^{3+} ions at the γ-Al_2O_3 surface are rapid enough to ensure that these sites will equilibrate within the 24-h preequilibration period. Therefore, we assume that near-surface Al^{3+} ions are present in octahedral coordination by amphoteric oxygen atoms (i.e., oxygen atoms bonded to zero, one, or two hydrogen atoms). The possible implications that surface transformation occurring during the sorption experiments might have on the kinetics of Cr(III) uptake will be discussed later. We refer to the preequilibrated γ-Al_2O_3 powder as alumina.

A $Cr(NO_3)_3 \cdot 9H_2O$ salt (Baxter) was used as the source for Cr(III) stock solutions in uptake experiments and XAFS sample preparation. All solutions were prepared with filtered, doubly deionized water, which had been stripped of dissolved CO_2 by boiling under a N_2 atmosphere. Solutions were prepared approximately 1 week prior to uptake experiments and XAFS sample preparation. All salts and standard solutions were reagent grade or better.

Uptake Measurements and XAFS Sample Preparation. Sample exposure to CO_2 was minimized by performing uptake experiments and XAFS sample preparation in a low CO_2 ($<10^{-7}$ atm) glovebox environment. Samples used to measure Cr(III) uptake as a function of pH and equilibration time were prepared from a single batch of preequilibrated, suspended alumina (10 g/L). These samples were prepared by delivering a 5-mL aliquot of the alumina slurry to an 8-mL polypropylene screw-top bottle. Initially, the suspension was titrated to pH 4 with approximately 65 μL of 0.1 N HNO_3. The suspension was allowed to equilibrate on an end-over-end rotator for 2 h. The sample was removed and placed on a stir-plate where a 2-mL aliquot of a Cr(III) stock solution ($[Cr]_i = 2$ mM), a predetermined amount of acid or base, and the necessary makeup water (0.1 M $NaNO_3$) to achieve a final volume of 8 mL were added to the suspension. The suspensions were placed back onto the rotator for 24 or 120 h. The suspension pH was measured at the end of the equilibration period with a double-junction glass electrode (Orion). The drift in pH during equilibration was less than one-tenth of a pH unit for all sorption samples. Supernatant solutions for quantitative Cr analyses were separated from the solid by passing the suspension through a 0.2-μm filter (VWR). Aqueous Cr concentrations were measured with a Perkin-Elmer 2000 flame and graphite furnace atomic absorption spectrometer. The amount of Cr associated with the alumina surface (i.e., uptake) was taken to be the difference between the total analyzed Cr concentration in a sample without alumina present (blank) and the analyzed concentration in the filtered supernatant solution. Surface coverage was normalized to surface area and is reported in units of $\mu mol/m^2$. Latti et al. (*15*) observed that the specific surface area of a dry γ-Al_2O_3 powder did not change after equilibrating in an aqueous solution for 1 month. Therefore, the surface area reported for the dry powder (100 m^2/g) was used in the conversion.

Each XAFS sample was prepared in an N_2 environment as a single titration experiment following the same procedure described above. Equilibration time refers to the time beginning when the target pH of the sample was reached and ending when the supernatant was separated from the solids. Solids for XAFS analysis were isolated by centrifugation. The wet-paste was then packed in a Teflon sample holder and covered with Mylar tape. The sample was wrapped in a moist paper towel and sealed in a Ziplock bag before it was removed from the glovebox and transferred to the beam-line. XAFS data collection began less than 1 h after centrifugation.

XAFS Data Collection and Analysis. Synchrotron-based XAFS measurements were performed at the Stanford Synchrotron Radiation Laboratory (SSRL) on beam lines IV-3 and IV-2 equipped with a Si(220) double-crystal monochromator. Fluorescence-yield Cr K-edge XAFS data were collected using either a Canberra Ge 13-element energy-dispersive detector or a Stern-Heald-type Ar gas-filled fluorescence detector fitted with a 3-μm Ti filter and solar slits to eliminate scatter (*19*). Higher-order harmonics in the incoming beam were removed with a Pt-coated mirror. This method of harmonic rejection minimizes the detuning of the monochromator crystals needed to completely eliminate harmonics.

Energy calibration was monitored by collecting the transmission spectrum of a chromium metal foil before and after each set of energy scans. The first inflection point of the K-edge of the chromium metal foil was assigned as 5989 eV. XAFS spectra were collected over the energy range of 5.7−7 keV. Averaging, normalization, and background subtraction of the raw XAFS spectra were performed with EXAFSPAK (*20*). Each averaged XAFS spectrum was separated into two regions, the X-ray absorption near-edge structure (XANES) spectral region and the extended XAFS (EXAFS) spectral region. XANES spectra (5960−6100 eV) were normalized and compared for qualitative information. EXAFS oscillations were isolated with a spline function and converted from energy to k-space ($k = 2m_e(E - E_0)/h^2$, where m_e is the mass of the electron, E is the energy, E_0 is the energy at $k = 0$, h is Planck's constant, and E_0 was defined as 6005 eV based on fits of Cr(III)-containing model compounds). Two to four transmission scans for model compounds and 10−15 fluorescence scans for sorption samples were collected out to $k = 12$ Å^{-1}. Beam-induced sample changes were not observed in the XANES or EXAFS region of sequential spectra for any of the samples, indicating no detectable change in oxidation state or coordination environment of Cr(III) during data collection.

Initially, the k^3-weighted EXAFS spectra of the model compounds γ-chromium(III) hydrous oxide, chromium(III) oxide, and uvarovite ($Ca_3Cr_2Si_3O_{12}$) were fit (k-range = 3−12 Å^{-1}) with phase shift and amplitude functions generated by FEFF7 (*21*). These fit results were used to test the theoretical phase shift and amplitude functions that were later used to fit unknown Cr(III) sorption samples. Values for coordination number (CN) and distance to scattering atoms (R) were determined from least-squares fits of the EXAFS and the Fourier-filtered EXAFS of each shell. The Debye−Waller values (σ^2) and the accuracy of parameters varied during the least-squares fits of solution and sorption samples (CN $\pm$

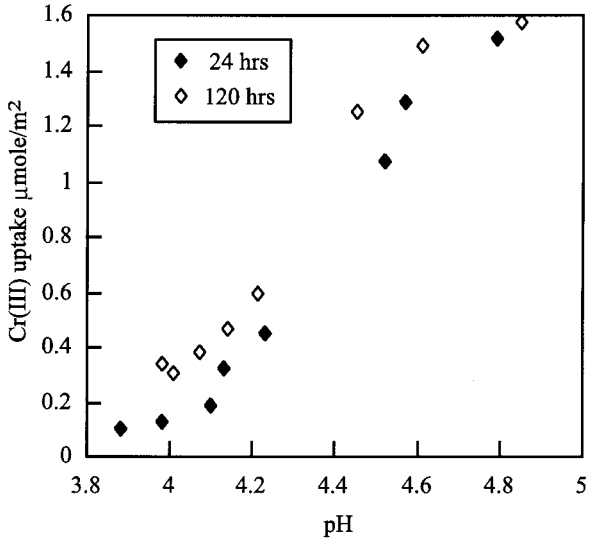

FIGURE 1. Cr(III) uptake on alumina during the period of slow uptake. Suspensions equilibrated for 24 h (closed symbols) and 120 h (open symbols) were prepared with 6.25 g/L alumina, $[Cr]_i = 0.5$ mM, and $[NaNO_3] = 0.1$ M.

10%, $R \pm 0.01$ Å 1st shell; CN ± 30%, $R \pm 0.02$ Å for more distant shells) were derived from a comparison of the fitted parameters of the model compounds with interatomic distances and coordination numbers reported in X-ray diffraction refinements of the structures of chromium(III) oxide (*22*) and uvarovite (*23*). Debye−Waller parameters were fixed to those derived during least-squares fitting of the EXAFS data of a structural model.

Results and Discussion

Cr(III) Uptake and Solution Speciation. The pH-dependent uptake of Cr(III) by alumina is shown in Figure 1 for sample equilibration times of 24 and 120 h. If it is assumed that Cr(III) ions adsorb only at surface functional groups (2.5 groups nm^{-2}) as monomers (*24*), then approximately 15% of these sites would be occupied at the highest surface coverage achieved in the time-dependent XAFS experiments (discussed below). The pH range over which adsorption proceeds from minimal uptake to complete removal of Cr(III) from solution (i.e., the adsorption edge) spans only a single pH unit. The shift of the adsorption edge to lower pH after equilibrating for 120 h indicates that Cr(III) uptake continues beyond 24 h. The shape of the adsorption edge does not change as a function of equilibration time in our experiments. The observed behavior is consistent with previous studies that found an initial period (<2 h) of rapid Cr(III) uptake (not indicated by the data shown in Figure 1) followed by a period of slow Cr(III) uptake by alumina (*4*, *5*).

To identify the possible aqueous reactants, the solution speciation of Cr(III) was characterized. If only Cr(III) monomers are considered, then thermodynamic constants predict that $Cr(H_2O)_6^{3+}$ (38%) and $Cr(H_2O)_5(OH)^{2+}$ (61%) should be the dominant Cr(III) hydrolysis products at the start of each titration. However, a number of authors have demonstrated that Cr(III) tends to form hydroxo polymeric species in aqueous solutions (*25*−*27*). Although there is some agreement in the literature on the formation constants of the first and second hydrolysis products of $Cr(H_2O)_6^{3+}$, a consensus regarding the occurrence, distribution, and kinetics of higher-order hydrolysis products, polymers, and hydroxide precipitates does not exist (*28*, *29*). It is important to note that these constants may not apply to the solution conditions of the current study because the chromatographic separation techniques and spectroscopic methods used to measure the

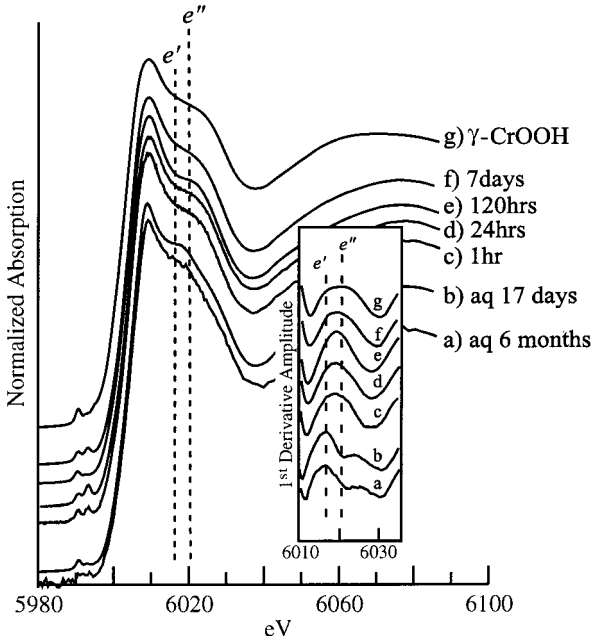

FIGURE 2. Background subtracted and normalized XANES spectra of Cr(III) in aged (a) and fresh (b) solutions, at the surface of alumina as a function of equilibration time (c−f), and in a homogeneous γ-CrOOH precipitate (g). e′ and e″ mark the electronic transitions characteristic of solution species and homogeneous precipitate, respectively. The inset contains the first derivative of each XANES spectrum.

distribution of polynuclear species require relatively concentrated Cr(III) solutions. Furthermore, because chromium(III) hydroxo polymeric species form slowly, solutions were typically equilibrated at high temperatures (50−75 °C). The few studies of solutions equilibrated at room temperature required long equilibration times (>100 days) to observe polymerization (*26*). Therefore, to avoid the uncertainty of using published formation constants and kinetic expressions to determine if chromium(III) hydroxo polymers should be considered as aqueous reactants, the speciation of Cr(III) was characterized in more concentrated and more aged solutions than those used in the sorption experiments.

The formation of chromium(III) hydroxo polymers in a 25 mM solution (50 times higher concentration than solutions used in the uptake experiments) was investigated as a function of solution aging. The XANES spectra of a solution aged at room temperature for 6 months and an equivalent solution equilibrated for 17 days are compared in Figure 2a and b. The 17-day equilibration time is relevant because at the completion of the longest sorption experiment, no more than 14 days had passed since the Cr(III) stock solution was prepared. The spectra are very similar. Most notably, the electronic transition labeled e′ in Figure 2 occurs at 6018 eV in both spectra. Unlike the XANES region, the EXAFS spectra (Figure 3a and b) of the two solutions and the corresponding Fourier transforms (Figure 4a and b) are significantly different. Both spectra are dominated by the backscattering contribution from the first coordination shell of six oxygen atoms at 1.97 ± 0.01 Å. However, the strong backscattering contribution from Cr(III) ions at 2.9 Å in the Fourier transform (uncorrected for phase shift) of the aged solution (Figure 4a) indicates that the local coordination environment beyond the first coordination shell has changed significantly during the 6 months of aging. The absence of a similar second shell contribution in the 17-day-old Cr(III) solution (Figure 4b) suggests that, within the sensitivity of the XAFS spectra, chromium(III) hydroxo polymers are not significant.

Local Coordination Environment of Cr(III) at the Alumina/Water Interface. The XANES spectra of Cr(III)

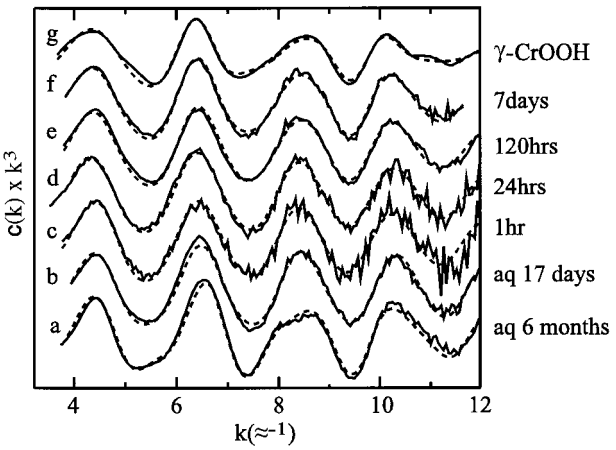

FIGURE 3. Cr K-edge, k^3-weighted EXAFS spectra (solid line) and least-squares fits (dashed line) of Cr(III) in aged (a) and fresh (b) solutions, at the surface of alumina at pH 4.3 as a function of equilibration time (c−f), and in a homogeneous γ-CrOOH precipitate (g).

adsorbed on alumina as a function of equilibration time are compared in Figure 2c−f. The absence of a sharp preedge feature at 5992 eV indicates that Cr predominantly occurs in the 3+ valence state in octahedral coordination in all of the samples shown (*30*). The XANES spectrum of adsorbed Cr(III) after equilibrating for 1 h (Figure 2c) differs from the aqueous Cr(III) spectrum (Figure 2b). Most notably, e′ (6017 eV in the Cr(III) aqueous spectrum) is observed at a higher energy (6019 eV) in the 1-h sorption sample spectrum. This feature continues to move to higher energy with increasing equilibration time, approaching e″ (6021 eV) in the γ-CrOOH spectrum (Figure 2g). An inset containing the 1st derivative of each XANES spectrum is included in Figure 2 to more clearly show this progression. A fundamental understanding of the structural significance of features in the XANES spectra is not well developed in such complex systems. However, the migration of this feature indicates that the coordination environment of Cr(III) is perturbed by the alumina surface after equilibrating for 1 h and that the predominant coordination environment of adsorbed Cr(III) continues to change with increasing equilibration time.

The EXAFS spectra of sorption samples shown in Figure 3c−f are dominated by a single oscillation, resulting from single scattering by the six oxygen atoms at 1.99 ± 0.01 Å that define the average Cr(III)$(O,OH,H_2O)_6$ octahedron. First shell oxygen atoms coordinated to Cr(III) ions adsorbed at the alumina/water interface may also be coordinated to protons (i.e., water molecules, hydroxide ions, or hydroxyl groups), Cr(III) ions (i.e., chromium hydroxo polymeric species), or Al ions (i.e., inner-sphere surface complex). Because backscattering amplitude scales with atomic number, backscattering by protons is not identifiable in EXAFS spectra. However, chromium(III) hydroxo polymers and inner-sphere complexes can be identified by contributions to the EXAFS from more distant shells of Cr or Al ions. In addition, the number of bonds to adjacent octahedra (i.e., corner-, edge- or face-sharing) can be inferred from the distance to Cr and Al shells (*31, 32*).

Scattering contributions to the EXAFS spectra from neighboring Cr and Al ions were isolated by subtracting the contribution from first shell oxygen atoms (i.e., what we refer to as the residual spectrum) and Fourier filtering the remaining spectral features between approximately 2.0 and 4.0 Å (uncorrected for phase shift). Parameters from least-squares fits of the Fourier-filtered residual (FFR) spectra were used as starting values in fits of the unfiltered EXAFS spectra. The final fit parameters shown in Table 1, which correspond to the least-squares fits of the unfiltered EXAFS spectra (dashed lines in Figure 3), are not significantly different from the starting values. The FFR spectra and their least-squares fits are shown in Figure 4. The FFR spectrum of aqueous Cr(III) monomers (Figure 4b) contains a single low-amplitude oscillation. Previous studies have fit this contribution with multiple scattering between the central Cr atom and O atoms within the octahedron and with single scattering from the second hydration shell (*33*). For the purposes of the current study, it is only important to point out that this contribution is not due to neighboring Cr atoms. The FFR spectrum after 1 h of equilibration with alumina (Figure 4c) has an additional contribution that was fit with approximately one Al atom at 2.88 ± 0.05 Å. After 24 h of equilibration, weak backscattering from Cr atoms at 2.97 Å also contributes to the FFR spectrum (Figure 4d). The phase and amplitude contributions to this spectrum from the Cr and Al shells are different enough that the correlation between Cr and Al coordination numbers is not significant. Noninteger coordination numbers reported in Table 1 may indicate that multiple Cr coordination environments are present at the alumina surface. For example, in the case of the 24-h sample, 0.6 Cr neighbors might indicate that only 25% of sorbed Cr is present as dimers and the remaining 75% is present as monomers. Although large uncertainties in the reported coordination numbers make this type of quantitative analysis speculative, this observation is useful. After even longer equilibration times, Cr atoms at 2.97 ± 0.01 and 3.93 ± 0.02 Å are required to fit the FFR spectra (Figure 4e,f). Attempts to fit the additional features in the EXAFS spectra with contributions from Al atoms were unsuccessful. Furthermore, the additional scattering amplitude from Cr atoms in EXAFS spectra of samples equilibrated for longer than 24 h appears to obscure the contribution from Al atoms; therefore, an Al shell is not included in the fits of these spectra. The dotted line overlaying the FFR spectrum of the "Hi 7 day" sample (Figure 4g) represents a fit that includes a shell of Al atoms at an edge-sharing distance (2.90 Å) in addition to the two shells of Cr atoms. The phase mismatch observed below $k = 9$ Å^{-1} was also observed for samples equilibrated for 120 h (Figure 4e) and 7 days (Figure 4f). The FFR spectrum of γ-CrOOH (Figure 4h) is composed of contributions from Cr atoms at approximately the same distances observed for the longest equilibrated sorption samples. However, even if a 4-fold increase in the Cr coverage is achieved by lowering the solid-to-liquid ratio (Figure 4g), the local coordination environment of sorbed Cr(III) ions is different from that in the homogeneous γ-CrOOH precipitate (Figure 4h). Previous EXAFS investigations demonstrated that Cr(III) surface precipitates are indistinguishable from the homogeneous γ-CrOOH precipitate (*7, 32*), although more recent Cr 2p, Fe 2p, and O 1s photemission and O K-edge absorption spectroscopy measurements on Cr(VI)-reacted Fe_3O_4(111) surfaces indicates that the chromium(III) hydroxide overlayer produced by reduction of the Cr(VI)(aq) is relatively disordered (*34*).

Adsorption, Polymerization, and Surface Precipitation. Although the composition and structure of the (hydr)oxide surface have been shown to influence the rate of sorption reactions (*12*), macroscopic uptake studies and pressure-jump experiments have established that metal ion sorption is generally characterized by a period of rapid uptake, followed by a period of slow uptake (*35, 36*). A cation can either associate with a (hydr)oxide surface through long-range forces (i.e., outer-sphere surface complex) or by forming direct chemical bond(s) with the surface (i.e., inner-sphere surface complex). Outer-sphere surface complexation has been proposed in similar systems when the XANES and EXAFS spectra of a sorbed metal ion are indistinguishable from the spectra of the metal ion in solution (*37*). After equilibrating for 1 h, the XANES and EXAFS regions indicate that Cr(III)

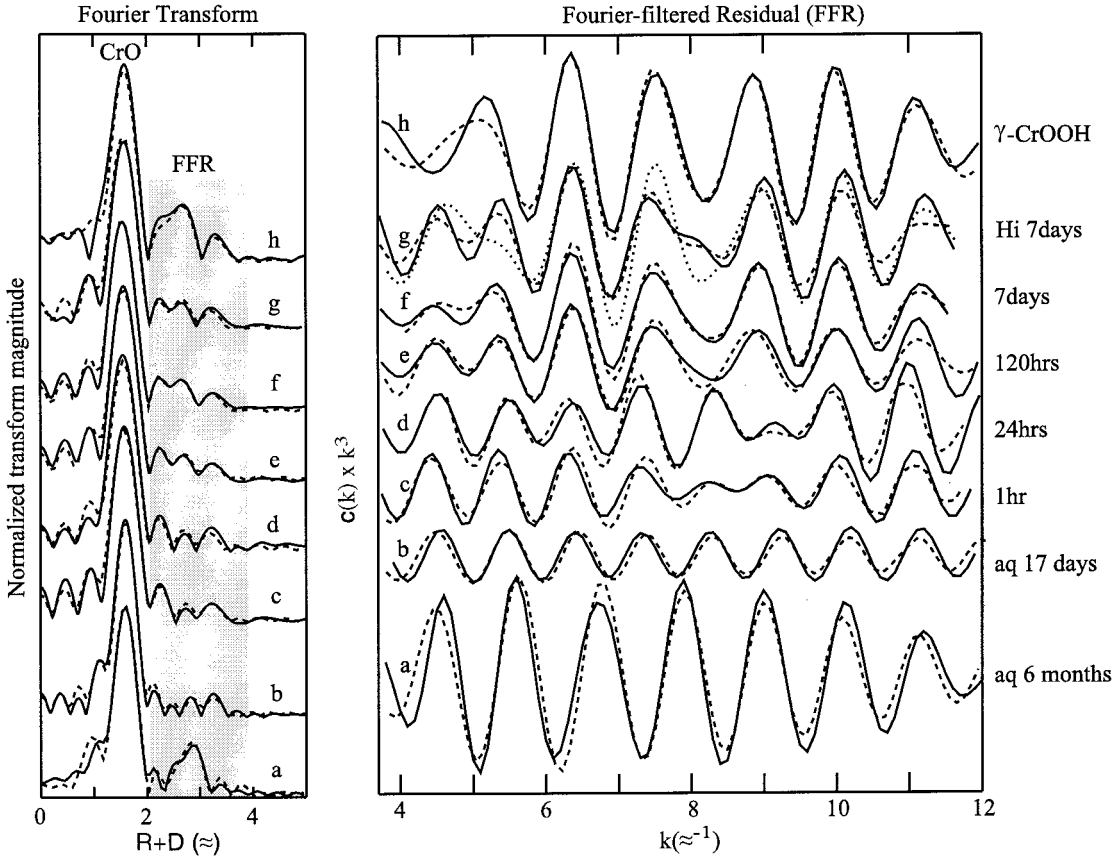

FIGURE 4. Normalized Fourier transforms (FTs) (uncorrected for phase shift) of EXAFS spectra (solid line) and least-squares fits (dashed line) shown in Figure 3. Fourier-filtered residual (FFR) spectra (solid line) were generated by back-transforming the region highlighted in the FTs after subtracting the scattering contribution from first-shell oxygen atoms. Parameters from the least-squares fits of the FFR spectra (dashed line) were used as seed values for fits of the EXAFS spectra. The dotted line overlaying the FFR spectra of the "Hi 7 days" samples (g) shows the fit quality when a shell of Al atoms is included at an edge-sharing distance. A Cr(III) coverage of 5.6 μmol/m^2 was achieved in the Hi 7 days sample by decreasing the solid-to-liquid ratio.

TABLE 1. EXAFS Fit Results[a]

	Cr−O		Cr−Al		Cr−Cr		Cr−Cr	
sample description	**CN**	***R* (Å)**	**CN**	***R* (Å)**	**CN**	***R* (Å)**	**CN**	***R* (Å)**
Cr^{3+}/γ-Al_2O_3 pH 4.3	±0.1[b]	±0.01[b]	±0.3	±0.03	±0.2	±0.02	±0.3	±0.04
1 h (0.23)[c]	5.9	2.00	1.1	2.87			0.6	3.94
24 h (0.41)	6.1	1.98	0.8	2.89	0.6	2.98	0.7	3.93
120 h (0.61)	5.7	1.99			1.1	2.98		
170 h (0.67)	5.6	1.99			1.5	2.96		
Cr^{3+}(aq) fresh[d]	6f	1.98						
Cr^{3+}(aq) aged[d]	6f	1.96			4.2	3.26		
γ-CrOOH(s)[e]	6f	1.99			2f	2.97	4.1	3.93

[a] Coordination number (CN) and interatomic distance (*R*) are listed for shells used in each fit. Parameter values followed by "f" were fixed based on fits of the Fourier-filtered data. Debye−Waller parameters were fixed at 0.004 (Cr−O) and 0.008 (Cr−Al and Cr−Cr shells) Å^2. [b] Estimated from least-squares fits of EXAFS spectra; error represents 95% confidence interval, 2σ. [c] Surface coverage in μmol/m^2. [d] Fresh and aged solutions were equilibrated at room temperature for 17 days and 6 months, respectively. [e] Isostructural with lepidocrocite (γ-FeOOH).

has already formed an inner-sphere complex at the alumina/water interface. In addition, the absence of backscattering from neighboring Cr(III) ions suggests that Cr(III) ions predominantly sorb as monomers. The distance to the shell of Al atoms (2.88 ± 0.05 Å) indicates that Cr(III) shares an edge with at least one $Al(O,OH)_6$ octahedron at the alumina/water interface. This type of complex requires that Cr(III) forms direct chemical bonds with at least two surface functional groups (surface functional groups are defined as oxygen atoms, hydroxyl groups, or water molecules bonded to at least one underlying Al atom) forming a bidentate monomeric Cr(III) complex of the type shown in Figure 5A.

The period of slow uptake is often attributed to metal ion diffusion into pores in the substrate, the surface substitution, or the formation of surface precipitates (*38*, *39*). If surface substitution were the dominant mechanism, then a greater contribution from neighboring Al atoms would be observed in the EXAFS spectra. Instead, Cr(III) neighbors are detected after 24 h of equilibration at a distance that is consistent with an edge-sharing dimeric $Cr_2(O,OH,H_2O)_{10}^{n-}$ complex. This Cr−Cr edge-sharing distance has been observed in other EXAFS investigations of Cr(III) sorption at metal (hydr)oxide/water interfaces (*7*, *32*). However, to the best of our knowledge, this result is unique in that the Cr−Cr edge-sharing distance has not been observed in the absence of a more distant shell of Cr(III) neighbors. The more distant shell of Cr(III) neighbors marks the formation of higher-order polymers or precipitates. Therefore, the data suggest that the dimer is the first polymeric species to form and that the dimers appear to form in the absence of precipitation. One

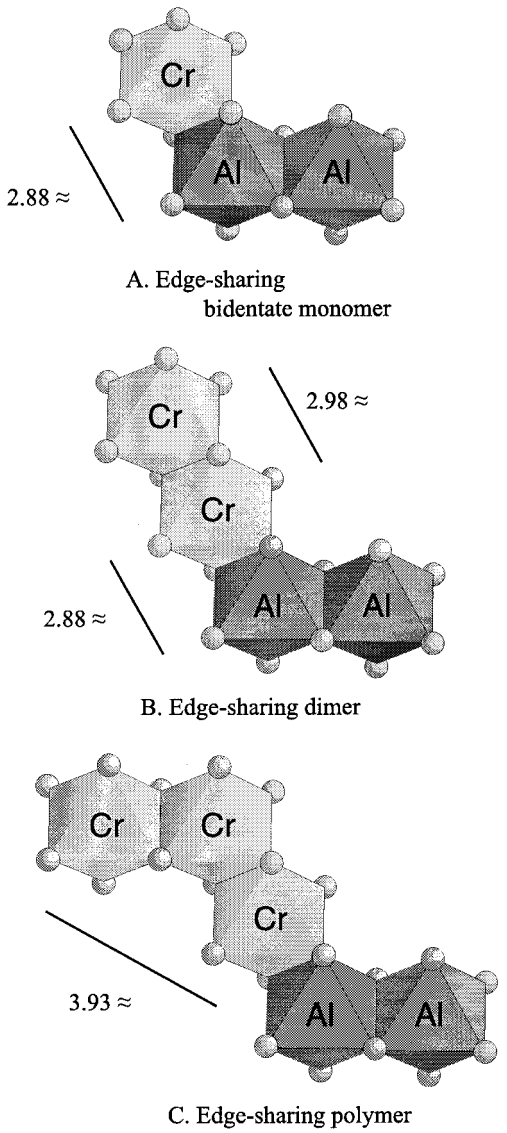

FIGURE 5. Polyhedral representation of proposed structural evolution of the predominant chromium(III) hydroxo species at the alumina surface with increasing equilibration time: (A) monomeric adsorption, (B) dimer formation, and (C) polymer formation.

possible arrangement of this type of surface complex is shown in Figure 5B.

The appearance of Cr atoms at 3.93 Å indicates that higher-order oligomers are present at the surface after longer equilibration times. The EXAFS spectra do not contain evidence for the formation of homogeneous chromium(III) hydroxide precipitates. Although the structural evidence in the EXAFS spectrum for precipitation may be obscured if poorly ordered precipitates are present (see, e.g., ref *34*), the XANES and EXAFS spectra of adsorbed Cr(III) and the homogeneous precipitate are clearly different (Figures 2 and 3). Another possible explanation for the appearance of neighboring metal atoms is that a mixed chromium(III)−aluminum(III) hydroxide precipitate or epitaxial overgrowth has formed and that the EXAFS spectra reflect the unique structure of this phase. Mixed chromium(III)−aluminum-(III) hydroxide precipitates have not been reported in the literature to the best of our knowledge. In addition, unlike previous observations of mixed-metal precipitates in other systems where distances to second and third shell metal ion neighbors are longer than in the pure hydroxide phase (*38, 40*), the near-neighbor Cr(III) distances observed in this study are consistent with edge-sharing chromium(III) hydroxo polymers and do not depend on equilibration time. The structural parameters provided by the EXAFS spectrum are consistent with the polymeric surface complex shown in Figure 5C.

Surface Complexation Reactions and Potential Uptake Mechanisms. The spectroscopic results indicate that the kinetics of Cr(III) uptake on alumina can be attributed to two distinct mechanisms. In the initial period of rapid uptake, $Cr(III)(O,OH,H_2O)_6^{n+}$ monomers form direct chemical bonds with at least two surface functional groups. The local coordination environment of this bidentate inner-sphere complex is consistent with the following reaction:

$$2AlOH + Cr(H_2O)_5(OH)^{2+} = (AlO)_2Cr(H_2O)_2(OH) + 2H_3O^+ \quad (1)$$

Heimstra et al. (*24*) used potentiometric titration data and structural constraints to propose that both singly and doubly protonated surface functional groups should be present at the alumina/water interface. To simplify the reaction, only the singly protonated or terminal surface functional group is represented in reaction 1. According to published hydrolysis constants, $Cr(H_2O)_6^{3+}$ and $Cr(H_2O)_5(OH)^{2+}$ are the dominant solution species under the conditions used in this study (*26*). The exchange rate of water molecules in the inner-coordination shell of the first hydrolysis product is 75 times greater than the exchange rate of water molecules coordinated to the fully protonated Cr^{3+} ion (*41*). Therefore, the reaction between the $Cr(H_2O)_5(OH)^{2+}$ species and surface functional groups is kinetically favored. The release of protons included in this reaction is consistent with potentiometric titrations, which indicate the release of two or three protons per adsorbed Cr(III) ion (*4*). However, the assumption that protons are released from the surface functional groups rather than from the hydration shell of the adion is speculative, and additional information about the structure of the reacting surface functional groups is required to further constrain protonation/deprotonation behavior.

We can infer from the fact that the rate of sorption decreases even when only a small percentage of surface sites is occupied by Cr(III) ions, that rapid uptake is limited to a subset of the total number of surface sites. Although it is possible that adsorption of Cr(III) monomers at additional sites formed as a result of alumina aging contributes to the slow uptake of Cr(III), the XAFS results suggest that once Cr(III) occupies these surface sites, a second sorption process becomes important whereby aqueous Cr(III) monomers react with sorbed Cr(III) to form edge-sharing dimeric species. The reaction during the period of slower uptake can be written as follows:

$$(AlO)_2Cr(H_2O)_3(OH) + Cr(H_2O)_5(OH)^{2+} = (AlO)_2Cr_2(OH)_4(H_2O)_4 + 2H_3O^+ \quad (2)$$

Once again, the rate of ligand exchange suggests that the first hydrolysis product is the dominant reactant. In analogous systems, the formation of an edge-sharing hydroxo-bridged species of the type represented in reaction 2 proceeds via a two-step process, where the singly bridged species exists as an intermediate species prior to forming the second hydroxo bond. However, Rotzinger et al. (*28*) suggested that the lifetime of the intermediate is probably too short to be a rate-limiting step in the proposed formation reaction. Alternatively, if the formation of the Cr(III) dimer is controlled by diffusion of Cr(III) monomers along the surface, then the reaction could be written with two adsorbed monomers as the reacting species. Eggleston and Stumm (*42*) observed Cr(III) surface diffusion and dimer formation on the (001) surface of α-Fe_2O_3 using scanning tunneling microscopy.

The XAFS investigations of Cr(III) solution speciation discussed above indicate that Cr(III) dimers do not form in solution within the time frame of the sorption experiments, even in more concentrated Cr(III) solutions where polymerization is observed at longer equilibration times. The proposed reaction sequence suggests that, following the period of rapid uptake, not only does Cr(III) prefer to bond to adsorbed Cr ions rather than the remaining unoccupied surface sites but also the alumina surface appears to enhance the rate of Cr(III) dimer formation. A possible explanation for the enhanced rate is provided by considering Cr(III) polymerization behavior in solution. The rate of Cr(III) polymerization in solution increases as the Cr(III) ion is hydrolyzed (*43*). Therefore, in addition to improving the odds of two Cr(III) ions coming together to form dimers, Cr(III) surface bonds appear to increase the lability of inner-coordination shell water molecules that are not bonded to the surface and thereby enhance Cr(III) polymerization.

Environmental Significance. Reactions 1 and 2 are indistinguishable from the point of view of proton release. However, the differences between monomeric sorption and polymerization have important implications for the kinetics of sorption, the sorption capacity of alumina, and the stability of Cr(III) sorption products at the alumina/water interface. In a contaminated aquifer where a continuous, subsaturated input of aqueous Cr(III) may exist, this study suggests that the reservoir available for Cr(III) removal from solution by (hydr)oxides is potentially far greater than the number of available surface active sites on alumina. Furthermore, to assess the stability of Cr(III) ions partitioned to metal (hydr)-oxides, it is necessary to consider the stability of Cr(III) monomers, polymers, and precipitates as a function of time. Brown et al. (*44*) demonstrated that a partition coefficient, K_d, used to predict the extent of Co(II) uptake on alumina strongly depends on whether monomeric sorption, polymerization, or precipitation is considered as the predominant uptake mechanism. The current study and the growing number of spectroscopic investigations of metal ion partitioning to metal (hydr)oxides, which suggest the interplay of multiple sorption mechanisms, demonstrate the importance of considering the full range of chemical reactions in the derivation of metal ion partitioning models.

Acknowledgments

We thank the staff of the Stanford Synchrotron Radiation Laboratory (SSRL) for their help and advice with the EXAFS experiments. We gratefully acknowledge the U.S. Department of Energy, Geosciences Program, for funding this work through Grant DE-FG03-93ER14347-A0007 and the DOE-EMSP Program through Grant DE-FG07-98ER14842. SSRL is supported by the Department of Energy (Division of Chemical Sciences and Materials Science and the Office of Biological and Environmental Research) and by the National Institutes of Health.

Literature Cited

(1) Chuan, M. C.; Liu, J. C. *Water Res.* **1996**, *4*, 932−938.
(2) Kimbrough, D. E.; Cohen, Y.; Winer, A. M.; Creelman, L.; Mabuni, C. *Crit. Rev. Environ. Sci. Technol.* **1999**, *29*, 1−46.
(3) Fendorf, S. E. *Geoderma* **1995**, *67*, 55−71.
(4) Wherli, B.; Ibric, S.; Stumm, W. *Colloids Surf.* **1990**, *51*, 77−88.
(5) Chang, K.-S.; Lin, C.-F.; Lee, D.-Y.; Lo, S.-L.; Yasunaga, T. *J. Colloid Interface Sci.* **1994**, *165*, 169−176.
(6) Fendorf, S. E.; Li, G.; Gunter, M. E. *Soil Sci. Soc. Am. J.* **1996**, *60*, 99−106.
(7) Fendorf, S. E.; Lamble, G. M.; Stapleton, M. G.; Kelley, M. J.; Sparks, D. L. *Environ. Sci. Technol.* **1994**, *28*, 284−289.
(8) Charlet, L.; Manceau, A. A. *J. Colloid Interface Sci.* **1992**, *148*, 443−458.
(9) Grolimund, D.; Kendelewicz, T.; Trainor, T. P.; Liu, P.; Fitts, J. P.; Chambers, S. A.; Brown, G. E., Jr. *J. Synchrotron Radiat.* **1999**, *6*, 618−620.
(10) Kendelewicz, T.; Liu, P.; Doyle, C. S.; Brown, G. E., Jr.; Nelson, E. J.; Chambers, S. A. *Surf. Sci.* **1999**, *424*, 219−231.
(11) Baumgarten, E.; Kirchhausen-Dusing, U. *J. Colloid Interface Sci.* **1997**, *194*, 1−9.
(12) Scheidegger, A. M.; Sparks, D. L. *Soil Sci.* **1996**, *161*, 813−831.
(13) Lasaga, A. C. Rate laws of chemical reactions. In *Kinetics of Geochemical Processes*; Lasaga, A. C.; Kirkpatrick, R. J., Eds.; MSA: Chelsea, MI, 1981; Vol. 8, pp 1−67.
(14) Karthein, R.; Motschi, H.; Schweiger, A.; Ibric, S.; Sulzberger, B.; Stumm, W. *Inorg. Chem.* **1991**, *30*, 1606−1611.
(15) Laiti, E.; Persson, P.; Oehman, L.-O. *Langmuir* **1998**, *14*, 825−831.
(16) Dyer, C.; Hendra, P. J.; Forsling, W.; Ranheimer, M. *Spectrochim. Acta* **1993**, *49A*, 691−705.
(17) Wijnja, H.; Schulthess, C. P. *Spectrochim. Acta* **1999**, *55A*, 861−872.
(18) Phillips, R. L.; Casey, W. H.; Karlsson, M. *Nature* **2000**, *404*, 379−382.
(19) Lytle, F. W.; Greegor, R. B.; Sandstrom, D. R.; Marques, D. R.; Wong, J.; Spiro, C. L.; Huffman, G. P.; Huggins, F. E. *Nucl. Instrum. Methods* **1984**, *226*, 542−548.
(20) George, G. N.; Pickering, I. J. *EXAFSPAK*; Stanford Synchrotron Radiation Laboratory: Stanford, CA, 1995.
(21) Ankudinov, A. L.; Ravel, B.; Rehr, J. J.; Conradson, S. D. *Phys. Rev. B* **1998**, *58*, 7565−7575.
(22) Newnham, R. E.; de Haan, Y. M. *Z. Kristallogr.* **1962**, *117*, 235−237.
(23) Novak, G. A.; Gibbs, G. V. *Am. Mineral.* **1971**, *56*, 791−825.
(24) Hiemstra, T.; Yong, H.; Van Riemsdijk, W. H. *Langmuir* **1999**, *15*, 5942−5955.
(25) Baes, C. B.; Mesmer, R. E. *The Hydrolysis of Cations*; Wiley: New York, 1976.
(26) Rai, D.; Sass, B. M.; Moore, D. A. *Inorg. Chem.* **1987**, *26*, 345−349.
(27) House, D. A. *Adv. Inorg. Chem.* **1997**, *44*, 341−373.
(28) Rotzinger, F. P.; Stunzi, H.; Marty, W. *Inorg. Chem.* **1986**, *25*, 489−495.
(29) Drljaca, A.; Spiccia, L. *Polyhedron* **1995**, *14*, 1653−1660.
(30) Peterson, M. L.; Brown, G. E., Jr.; Parks, G. A. *Colloids Surf. A* **1996**, *107*, 77−88.
(31) Cheah, S.-F.; Brown, G. E., Jr.; Parks, G. A. *J. Colloid Interface Sci.* **1998**, *208*, 110−128.
(32) Manceau, A.; Charlet, L. *J. Colloid Interface Sci.* **1992**, *148*, 425−442.
(33) Lindquvist-Reis, P.; Munoz-Paez, A.; Diaz-Moreno, S.; Pattanaik, S.; Persson, I.; Sandstrom, M. *Inorg. Chem.* **1998**, *37*, 6675−6683.
(34) Kendelewicz, T.; Liu, P.; Doyle, C. S.; Brown, G. E., Jr. *Surf. Sci.*, in press.
(35) Hayes, K. L.; Leckie, J. O. *J. Colloid Interface Sci.* **1987**, *115*, 564−572.
(36) Sparks, D. L.; Scheidegger, A. M.; Strawn, D. G.; Scheckel, K. G. In *Mineral−Water Interfacial Reactions: Kinetics and Mechanisms*; Sparks, D. L., Gundl, T. J., Eds.; American Chemical Society: Washington, DC, 1998; Vol. 715, pp 108−135.
(37) Hayes, K. F.; Roe, A. L.; Brown, G. E., Jr.; Hodgson, K. O.; Leckie, J. O.; Parks, G. A. *Science* **1987**, *238*, 783−786.
(38) Thompson, H. A.; Parks, G. A.; Brown, G. E., Jr. *Geochim. Cosmochim. Acta* **1999**, *63*, 1767−1778.
(39) Scheidegger, A. M.; Strawn, D. G.; Lamble, G. M.; Sparks, D. L. *Geochim. Cosmochim. Acta* **1998**, *62*, 2233−2245.
(40) Scheidegger, A. M.; Lamble, G. M.; Sparks, D. L. *Environ. Sci. Technol.* **1996**, *30*, 548−554.
(41) Xu, F.-C.; Krouse, H. R.; Swaddle, T. W. *Inorg. Chem.* **1985**, *24*, 267−270.
(42) Eggleston, C. M.; Stumm, W. *Geochim. Cosmochim. Acta* **1993**, *57*, 4843−4850.
(43) Crimp, S. J.; Spiccia, L.; Krouse, H. R.; Swaddle, T. W. *Inorg. Chem.* **1994**, *33*, 465−470.
(44) Brown, G. E., Jr.; Parks, G. A.; Bargar, J. R.; Towle, S. N. In *Mineral−Water Interfacial Reactions: Kinetics and Mechanisms*; Sparks, D. L., Gundl, T. J., Eds.; American Chemical Society: Washington, DC, 1998; Vol. 715, pp 14−36.

Received for review December 22, 1999. Revised manuscript received September 5, 2000. Accepted September 5, 2000.

ES9914285